Disponible en www.hormigonyacero.com
Hormigón y Acero, 2025
https://doi.org/10.33586/hya.2025.4148

ARTÍCULO EN AVANCE ON LINE

A Preliminary Approach for Accidental Load Design of a Submerged Floating Tube Bridges: Blast-Fire Interaction on RC Slabs

Colombo, M., Arano, A., di Prisco, M, Hendriks, M. A. N., Kanstad, T., Martinelli, P., Minoretti A, Øverli, J. A.

DOI: https://doi.org/10.33586/hya.2025.4148

Para ser publicado en: *Hormigón y Acero*

Por favor, el presente artículo debe ser citado así:
Colombo, M., Arano, A., di Prisco, M, Hendriks, M. A. N., Kanstad, T., Martinelli, P., Minoretti A, Øverli, J. A. (2025) A Preliminary Approach for Accidental Load Design of a Submerged Floating Tube Bridges: Blast-Fire Interaction on RC Slabs, *Hormigón y acero*, https://doi.org/10.33586/hya.2025.4148

A preliminary approach for accidental load design of a submerged floating tube bridges: blast-fire interaction on RC slabs

Colombo, M.[(1)], Arano, A.[(2)], di Prisco, M.[(1)], Hendriks, M. A. N.[(3,4)], Kanstad, T.[(3)], Martinelli, P.[(1)], Minoretti A.[(3, 5)], Øverli, J. A.[(3)]

(1) Politecnico di Milano – Milan – Italy
(2) Former NTNU – Trondheim – Norway
(3) NTNU – Trondheim – Norway
(4) TU Delft – Delft – Netherlands
(5) Statens vegvesen Utbygging (Norwegian Public Road Administration) – Trondheim Norway

ABSTRACT

Submerged floating tunnels are more and more considered as a suitable solution to cross water channels limiting environmental impact on the visual landscape and ensuring large ship passage while crossing large distances between coasts. The design of this kind of strategical infrastructures must deal not only with live loads and particular loading condition coming from the floating situation but needs also to carefully consider accidental actions that concur to the global safety of the infrastructure. The construction of the new E39 highway along the Norwegian coast asks for crossing several fjords and this solution is seriously taken into consideration. For this reason, a comprehensive research programme was aimed at the analysis of accidental load design of the infrastructure. This paper aims to present a comprehensive overview of an ad-hoc experimental investigation on the behaviour of reinforced concrete (RC) circular slabs (60 cm diameter) under exposure to fire, blast, or a combination of both actions. Additionally, it seeks to draw design-driven conclusions that could be valuable for the design of critical infrastructure in scenarios involving fire and blast. The presented experimental campaign was intended to provide a benchmark for assessing the reliability of the design approaches to be adopted in the design of the global infrastructure. First, the concrete mechanical characterisation at normal condition and at high temperatures was performed referring both to the uniaxial compression and uniaxial tension. The structural behaviour of simply supported RC

slab has been also investigated by considering slabs exposed to a hydrocarbon fire curve at different exposure times and by considering the post-fire application of static or dynamic loading condition. In particular, the fire curve was applied by a gas burner while the dynamic load was reproduced by a shock tube equipment that was used to apply two different blast-like pressure histories.

Keywords: Submerged floating tunnel; Concrete mechanical properties; Fire exposure; Blast loading; High temperatures; RC slabs; Fire-blast interaction

1. Introduction

Reinforced concrete (RC) structures represent the major part of today's infrastructure, for example in bridges and tunnels. In addition to the normal design loadings, RC structures may be exposed to extreme hazards throughout their service life, including accidental actions (fire exposure and blast as a consequence of fire in case of goods transport), natural disasters (earthquakes) or even terrorist attacks (Zhai et al. 2016, Ruan et al. 2015). This can cause a huge deterioration of the structure, affecting both the serviceability and the structural resistance.

In the case of tunnels, the consequences of extreme events can be even worse due to the relative closedness of the structure, especially concerning the effects related to fire exposure which is often regarded as the main physical threat in their design. Disastrous fire events in tunnels in Europe, e.g. Mont Blanc Tunnel (1999), Gotthard Tunnel (2001), Tauern Tunnel (2002), Frejus Tunnel (2005), and Viamala Tunnel (2006), have increased the attention paid to safety issues in these types of structures, underlining the importance of investigating these infrastructures from human and economical points of view. However, nowadays fire can no longer be considered alone when evaluating extreme actions, considering recent terrorist attacks or tragic accidents. An explosion after a fire exposure may lead to potentially disastrous consequences, easily aggravating the damage in the structure or even causing the complete collapse (Zhang et al. 2019, Colombo et al. 2021). The tragic collision which recently occurred in Casalecchio, Italy (2018), can be regarded as an example of this kind of scenario. Two trucks loaded with flammable materials triggered a chain of explosions that gutted an overpass infrastructure, causing two deaths and 145 injuries.

The investigation of the combined action of fire and explosion loads in tunnels is of great interest also for the Norwegian Public Roads Administration's (NPRA) E39 coastal highway route project. This project is aimed at establishing an improved, and potentially ferry-free, highway route between Kristiansand to Trondheim along the Norwegian west coast,

reducing the travel time by half (Børre and Minoretti 2014). To do so, this pioneering project needs to evaluate many fjord crossings, including seven ferry connections. Conventional bridges or undersea tunnels can be used as fixed connections for many of the fjord crossings. However, the uncommon dimensions of some fjords like Sulafjorden, which is 5 km wide and more than 1 km deep, make these conventional structures not feasible. Alternative solutions therefore need to be considered, as for example floating bridges or submerged floating tunnels also known as submerged floating tube bridges (SFTB) (Minoretti et al. 2020). Figure 1a shows a comparison of different fjord crossing alternatives.

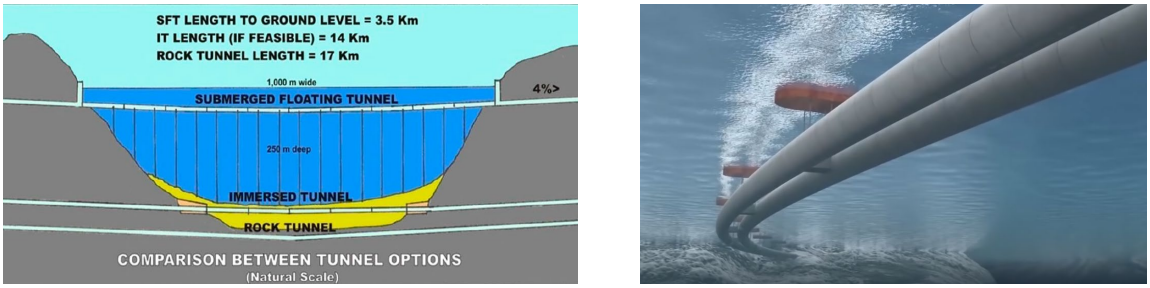

(a) (b)

Figure 1. (a) Different crossing alternatives (Minoretti et al. 2020); and (b) sketch of the submerged floating tube bridge for the Sognefjord crossing (Statens vegvesen)

The SFTB is a type of floating bridge (*fib* Bulletin 96, 2020), submerged at a defined position under the sea level, see Figure 1b. In the case of deep fjords, the depth of the SFTB allows to optimize the length of the crossing, compared to traditional undersea tunnels (Figure 1a). The research studies promoted by the NPRA, in conjunction with the advanced offshore technology available in Norway, have now demonstrated the feasibility of the SFTB (Minoretti et al. 2020). Nevertheless, ongoing research projects are still oriented toward investigating safety considerations to ensure robustness and redundancy for the whole structure. The specific scenario of the combined action of fire and subsequent internal explosion, illustrated in Figure 2, represents a crucial safety design condition for this structure. The limited data available on

the combined effect of such two extreme loads makes the study of this accidental scenario a great engineering challenge (Minoretti et al. 2020)

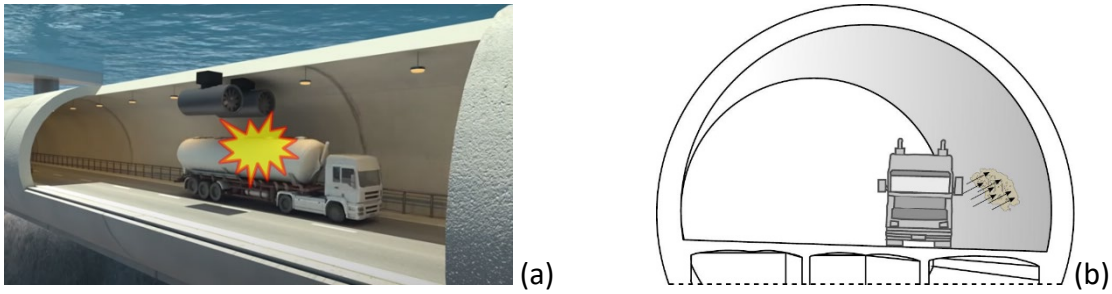

Figure 2. (a) Accidental scenario of fire and blast loads; and (b) sketch of the SFTB cross-section

Large-scale experimental tests on RC structures are uncommon due to the huge cost and testing difficulties. In fact, there are limited experimental studies reported in the literature investigating tunnels subjected to internal blast loads at present (Kristoffersen et al. 2021). Small-scale tests in RC concrete members, such as slabs, beams, or tunnel linings, are alternatively carried out. The accidental loads are reproduced in such elements, to some extent, and their structural behaviour is then investigated with the objective of assessing the scenario in full-scale structures. In a common tunnel serviceability condition, a compressive membrane state of stress is the most important action. Nevertheless, when an accidental action hits the tunnel, non-symmetric load condition can be applied to the structure thus leading to bending action that could drive the global failure of the structure. For this reason, RC slabs can be considered as reference elements to be investigated.

The assessment of a complex structure under an extreme load condition typically requires advanced numerical models. These models often need to be validated comparing their predictions with the results from experimental tests. The experimental findings of this study are therefore valuable to define a reliable benchmark for numerical models which, with numerical upscaling, will be instrumental for the design of the SFTB under exceptional load conditions, such as the combined action of fire and subsequent blast loading.

2. Research significance

This study experimentally investigates the combined effect of fire exposure and blast loading on RC slabs. Figure 3 shows the research strategy for the investigated case scenario, illustrating the scope of this study within the background project and the future research. As seen, the study comprises material tests on concrete cylinders, and fire tests in combination with static and dynamic tests on RC circular slabs. The findings of this study are relevant for assessing the reliability of the numerical models that will later be used in the design of SFTBs.

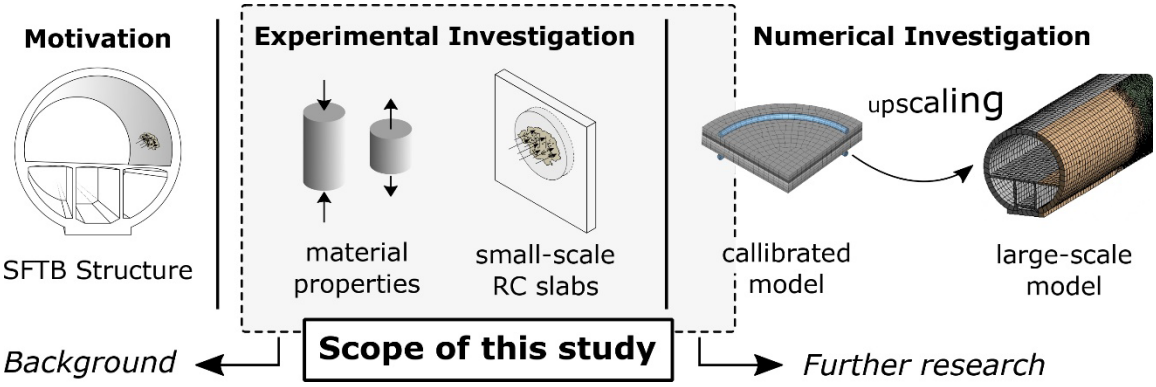

Figure 3. General overview of the research

The investigation of RC slabs subjected to fire and blast comprises a broad field. Some of the topics that fall out of the present research study are here mentioned. Concerning the material testing, the effects of elevated temperatures on the specific concrete mix intended to be used in future SFTB structures are investigated. The behaviour of the material is evaluated at a macro level, where the changes at a smaller meso- or micro-structural level are not addressed. In addition, the dynamic behaviour of this type of concrete subjected to high strain rates was not investigated. Concerning the experiments on RC circular slabs, one geometry configuration is studied, dictated by the dimensions of the experimental device to be used. Effects of different reinforcement ratios, thicknesses or concrete covers are therefore not addressed. The fire exposure applied on the slabs is the hydrocarbon fire curve with two different fire exposure times. Two different pressure levels are considered in the dynamic tests.

This study focuses on two main objectives:

- To provide experimental data on the high-temperature mechanical properties of materials, which can serve as input for implementing a detailed material model in the development of an advanced numerical simulation. The materials used in the experimental program—and thus the resulting data—are highly representative, as they correspond to those considered in the preliminary design of the E39 SFTB.
- To establish a reliable structural benchmark for calibrating numerical models. Although the geometry of the test specimens does not directly match that of the SFTB, the experimental tests serve as a realistic benchmark. This is because they are designed to reproduce a structural response—slab biaxial bending—that could occur during a potential internal accident within the tunnel shell. As illustrated in Figure 2, an internal explosion could result in a non-uniform pressure distribution, causing local bending of the tunnel structure.

In the final stage, a large-scale model of the entire structure can be developed, accounting for upscaling effects, to investigate different accidental scenarios and thus assess the safety in the design of the SFTBs in the *E39 coastal highway route* project.

3. Experimental campaign overview

The experimental campaign summarized in this paper refers, as already discussed, to the investigation of the bending behaviour of reinforced concrete slabs subjected to fire and/or blast action. The material is a concrete of grade C45/55 which today represents typical concrete used in Norwegian infrastructures under exposed conditions. The density of the concrete was equal to 2370 kg/m^3 and the average measured cylindrical compressive strength is equal to 73 MPa. A water-cement ratio of 0.42 was considered with a maximum aggregate size of 16 mm. Polypropylene microfibres were also added to the mix (1 kg/m^3) solely to prevent explosive

spalling, not for their tensile contribution. The complete mix design is provided in Table 1.

The structural elements investigated consist of reinforced concrete circular slabs, 70 mm thick, with a diameter of 690 mm. The specimen sizes are detailed in Figure 4. Two layers of bi-directional reinforcement (Ø6/60 mm both in x and y direction) were positioned as shown in Figure 4a-b. A minimum concrete cover of 10 mm was used.

The steel reinforcement used is B450, with an average yield strength of 500.8 MPa and an average ultimate strength of 684.8 MPa, experimentally determined in accordance with the ISO 15630-1 (2019) procedure.

The overall experimental campaign is made of three different phases:

- Detailed material characterization in normal condition and after exposure to high temperature.
- Static bending tests on slabs exposed to fire action.
- Bending tests of slabs exposed to fire action and loaded with shock wave.

Table 1 Concrete mix proportions per cubic meter

Component	Content (kg/m^3)
CEM II/B-M 42.5R	223.40
CEM II/A-V 42.5N	193.33
Silica fume	12.89
Water	174.13
Aggregate 8–16	754.95
Aggregate 0–8	1026.48
Acrylic superplasticizer	3.06
Set-retarding admixture	0.64
Polypropylene fibres	1.00

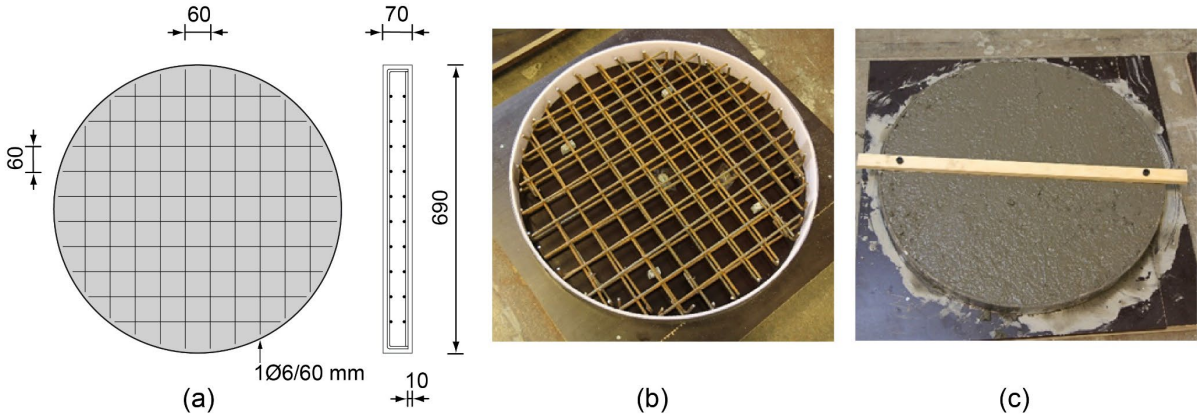

Figure 4. (a) Slab specimen geometry and (b,c) images of casting phases (reprinted with permission of the publisher – Colombo et al. 2021)

4. Material properties at high temperatures

A proper definition of the material properties is a basic precondition of a reliable numerical model. A complete overview is rarely available in the literature, where only the basic properties, such as the compressive strength and the modulus of elasticity, are typically investigated. For this reason, the effect of elevated temperatures on the mechanical behaviour of concrete was experimentally investigated on concrete cylinders in residual conditions, after a single thermal cycle at different elevated temperatures (200, 400 and 600 °C), also including some results at 800 °C (Arano et al. 2021). Since concrete degradation is primarily governed by the maximum temperature reached rather than the instantaneous temperature, residual tests—where the material is tested at room temperature after undergoing a thermal cycle—are generally considered a reliable method for evaluating the high-temperature properties of concrete. This approach is also supported by the findings of Felicetti and Gambarova (1998, 1999) and Felicetti et al. (2000).

The obtained complete compressive and tensile constitutive responses of concrete are represented in Figure 5a and in Figure 6a respectively and allowed to calculate additional material parameters such as the fracture energy, peak strength and peak deformation or crack opening and their evolution at high temperatures (Figure 5b and Figure 6b).

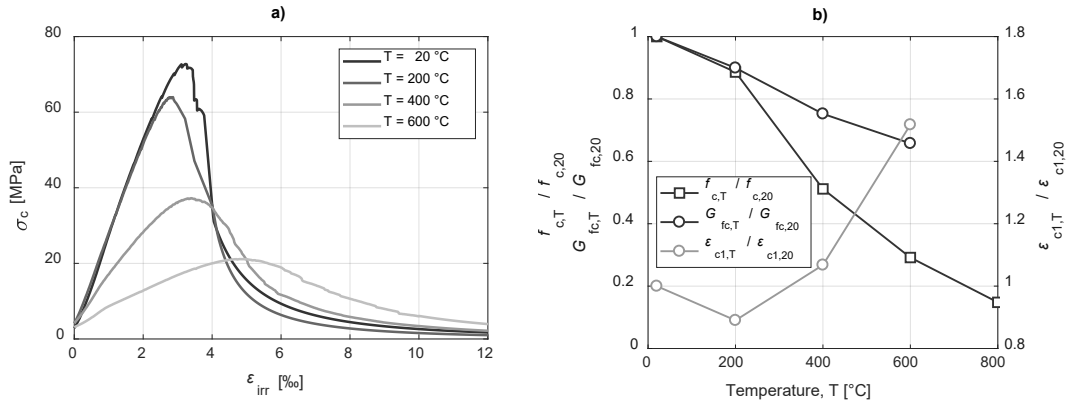

Figure 5. (a) Average compressive stress-strain curves, and (b) evolution of nominal compressive peak strength, specific compressive fracture energy, and strain at peak stress, after cooling (extracted from Arano et al. 2021)

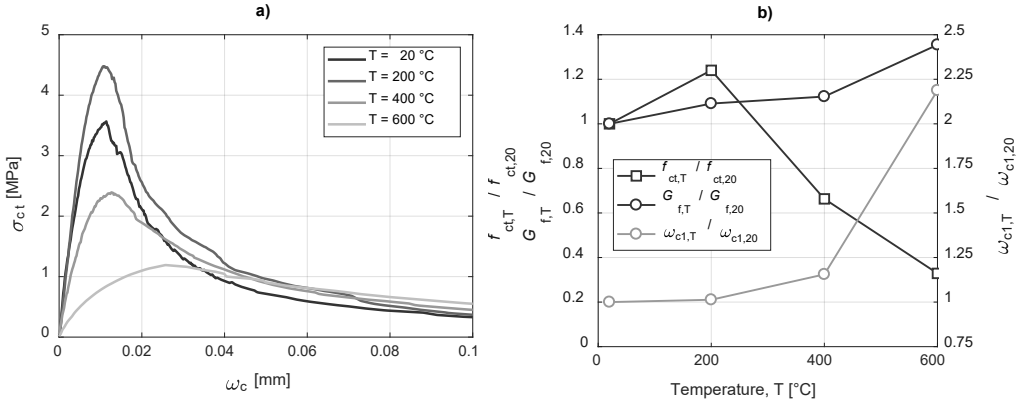

Figure 6. (a) Average tensile stress-crack opening curves, and (b) evolution of tensile nominal peak strength, specific tensile fracture energy, and crack opening at peak stress after cooling (extracted from Arano et al. 2021)

A comparison with previous research studies available in the literature and Standards (prEN 1992-1-2, 2019; *fib* Model Code 2010, 2013) confirmed the negative effect that elevated temperatures cause on the basic mechanical properties of concrete. The relationships of mechanical properties at high temperatures proposed in the new version of the Eurocode 2-Part 1-2 (2019) partially agree with the experimental findings, even though a large scatter in the results was found in the literature (Figures 7, 8). The relationships presented by the *fib* Model Code 2010 (2013) and Nakamura and Higai (2001) of the specific tensile and compressive

fracture energy (Figures 9, 10) respectively are not meant to, and should not, be used at high temperature, as they yield inaccurate results.

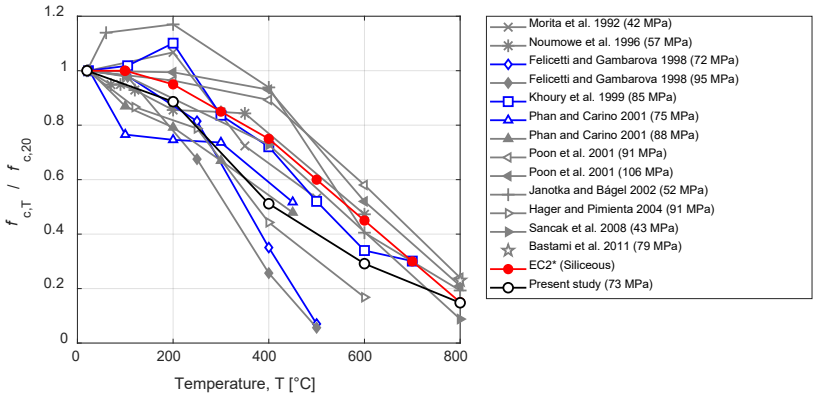

Figure 7. Evolution of the uniaxial compressive strength with temperature (extracted from Arano et al. 2021)

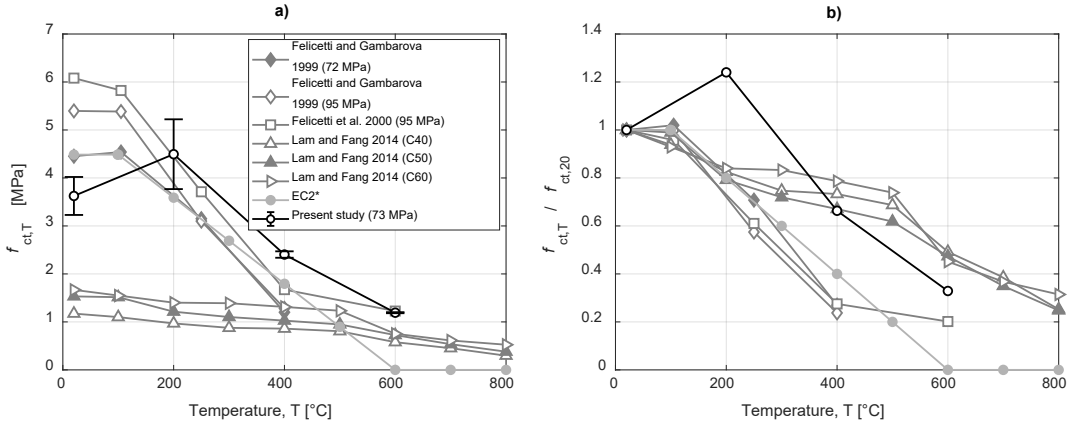

Figure 8. Evolution of the uniaxial tensile strength with temperature (extracted from Arano et al. 2021)

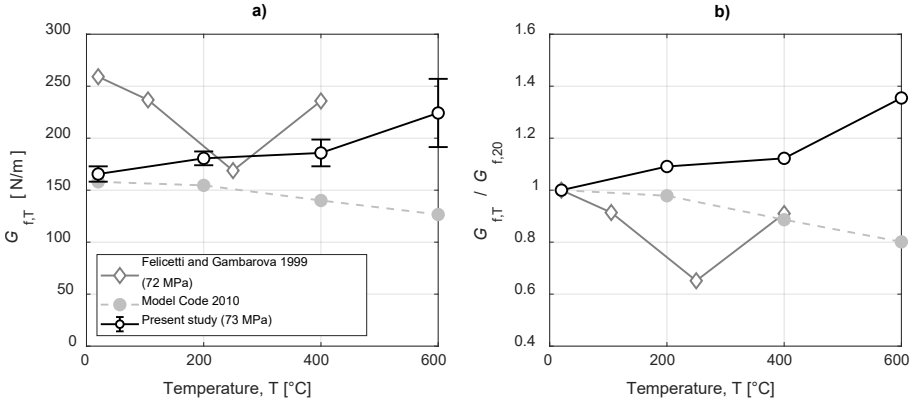

Figure 9. Evolution of the tensile fracture energy with temperature (extracted from Arano et al. 2021)

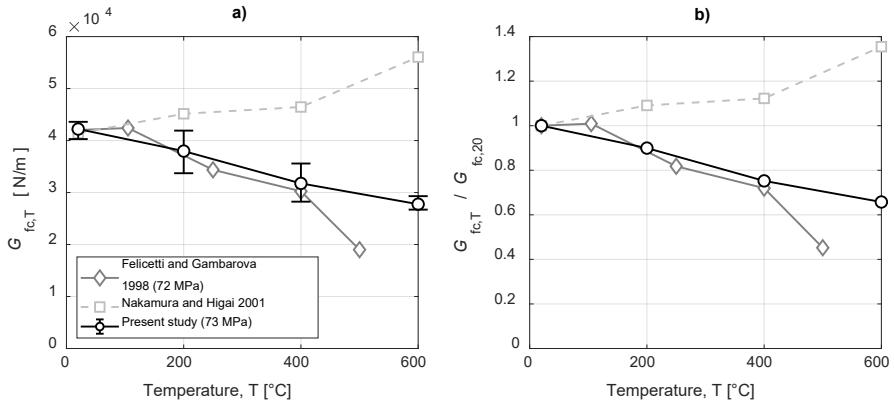

Figure 10. Evolution of the compression fracture energy with temperature (extracted from Arano et al. 2021)

Results from the comprehensive experimental approach presented can be instrumental to the parameter definition and calibration of common constitutive models for concrete, increasing accuracy on the prediction of the structural behaviour. In addition, results from basic properties may contribute to the already available data from the literature, where discrepancies between research studies are reported.

5. Static behaviour of slabs in case of fire exposure

The characterization of the material behaviour at high temperatures does not provide a complete description of the structural response of a member subjected to fire, since other effects, such as reinforcement or stress redistribution, need to be considered. In the present programme, the effect of fire exposure on the static structural response of RC slabs was investigated (Arano et al. 2023). A hydrocarbon fire curve was applied to the slab by means of a gas burner, studying two fire exposure times (60 and 120 min) in addition to the reference (unexposed) case. The gas burner was placed in front of the sample (Figure 11) and some thermocouples were introduced during casting to monitor the temperature distribution through the sample thickness.

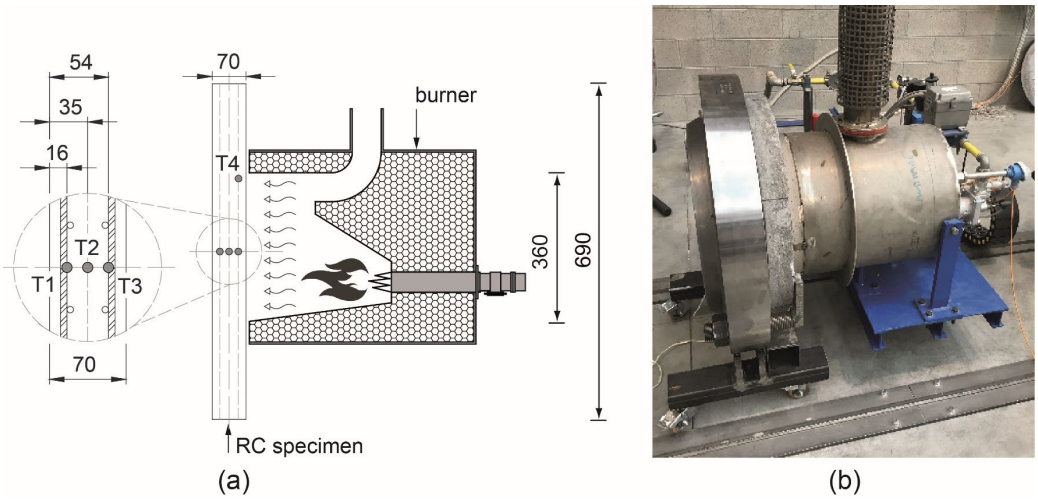

Figure 11. Experimental set-up for fire application (reprinted with permission of the publisher – Colombo et al. 2021)

The main objective was to evaluate the effect of fire exposure on the load-bearing response of the slab. Simplified mechanical models (including the yield-line approach) were used to discuss the obtained experimental results. Thermocouples embedded in the specimen and an ultrasonic pulse velocity (UPV) equipment, enabled to study the effect of high temperatures across the thickness, thus evaluating the decrease of the overall stiffness of the slab. The temperature profile across the slab thickness is shown in Figure 12(a, b). The same figure, parts (c) and (d), displays the heated surface of two reference samples after exposure to the fire curve. The colour change of the material, visible in the images, reflects the maximum temperature reached during fire exposure, as also noted by Colombo and Felicetti (2007).

A static bending test was performed on each slab after it had cooled down to room temperature following fire exposure. It is important to note that in concrete materials and structures, damage is primarily governed by the maximum temperature reached rather than the instantaneous temperature. Furthermore, during the cooling phase, the temperature of the inner layers can increase due to convection–diffusion processes, resulting in a higher internal temperature compared to the instantaneous profile observed at the end of a defined fire

exposure. For these reasons, although the testing procedure does not perfectly replicate real conditions, it is considered reliable—and even conservative from a safety perspective.

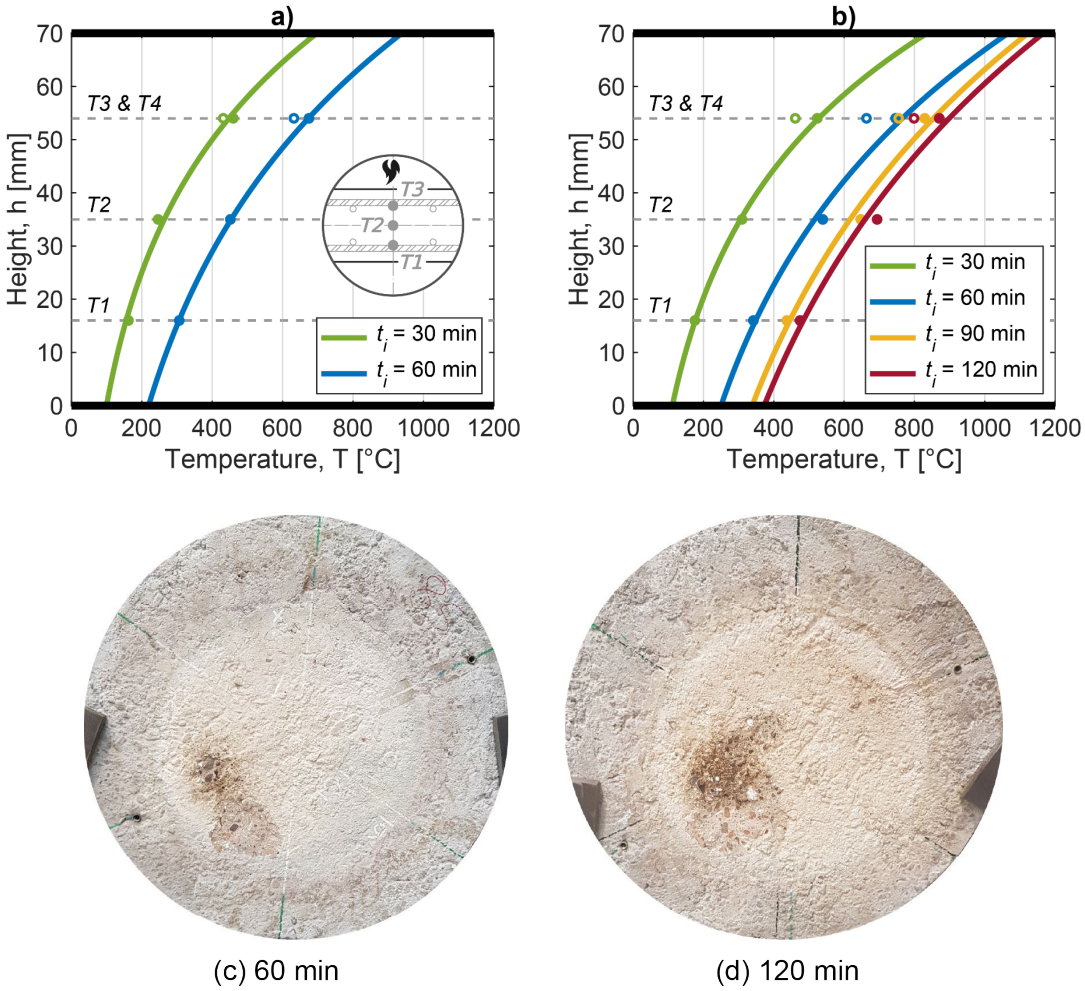

Figure 12. (a, b) Temperature profile during hydrocarbon fire curve application (reprinted with permission from the publisher – Arano et al., 2023); (c, d) Images of the heated surface of the samples after fire exposure (c – sample S8, d – sample S7).

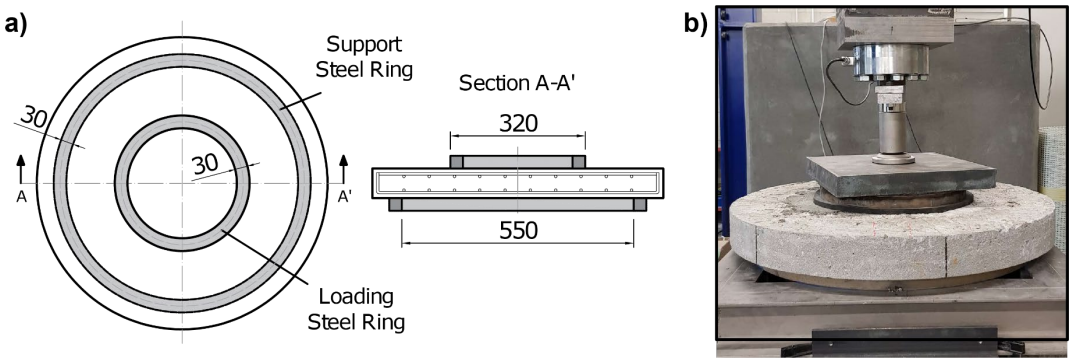

Figure 13. Experimental set-up for the static bending tests on slabs (reprinted with the permission of the publisher – Arano et al. 2023)

The tests were displacement-controlled using an electromechanical jack with a maximum capacity of 400 kN. The displacement rate was 50 μm/s up to a load of 100 kN, and 80 μm/s up to failure. The vertical deflection of the specimens was measured using a linear variable differential transformer (LVDT) positioned at the centre of the rear surface.

A circular steel ring with a major diameter of 320 mm was used to apply the load. The specimens were loaded on the surface that had previously been exposed to fire (the top surface during casting). A thin layer of neoprene was placed under the loading ring to distribute the load at the contact point between the steel ring and the specimen surface. The specimens were simply supported on a circular steel ring with a minor diameter of 550 mm. Both rings had a radial thickness of 30 mm. Figure 13 illustrates the setup for the static tests.

The dimensions of the support ring were selected based on the support scheme for the dynamic tests discussed later. For this reason, no neoprene layer was placed between the slab surface and the support ring. In the dynamic tests, the load is applied as a pressure wave, that is, a uniformly distributed load on the slab surface. Due to the difficulty of reproducing a uniformly distributed load under displacement control in a static test, the equivalent linear ring load was adopted to delay punching failure, which would typically result from a concentrated load.

Results of the load-deflection response are represented in Figure 14 in terms of load vs. central deflection. The curves showed two main peak loads, corresponding to two different structural mechanisms. A stiffer peak was first obtained through an arch mechanism, caused by the specific set-up used in the tests, which enhanced the bending capacity. The arch peak load was considerably reduced after the fire exposure, due to the negative effect on the concrete mechanical behaviour. At large deflections, the tensile membrane action (TMA) enhanced the ultimate load reached. Unlike the arch peak load, the ultimate load was not significantly influenced by the exposure to high temperature mainly due to the strong recovery of steel after

cooling, confirming the robustness and structural reliability of this RC slab in residual conditions.

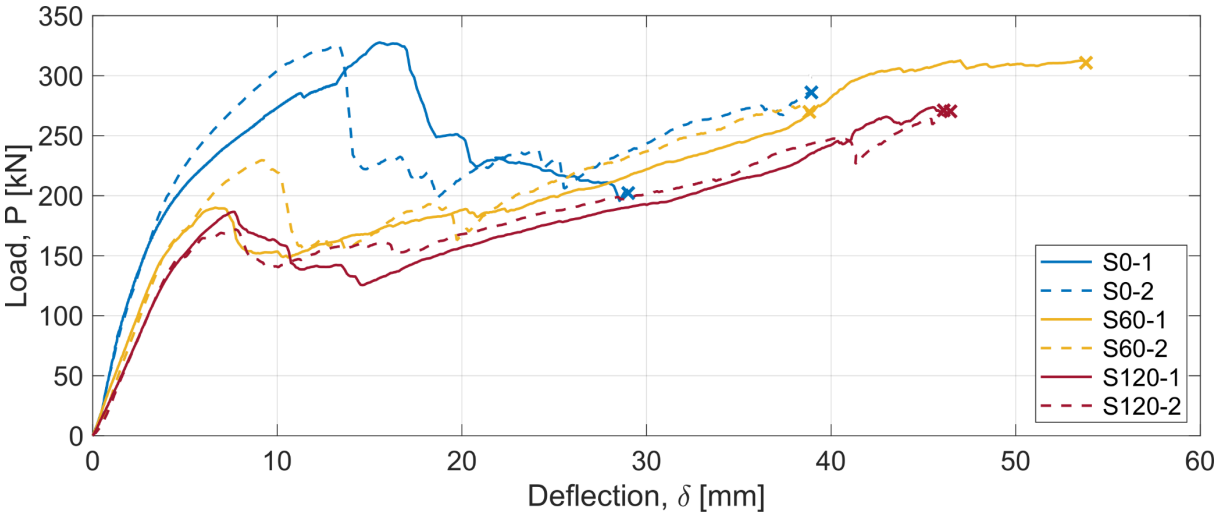

Figure 14. Experimental results of the static bending scheme on slabs (Reprinted with the permission of the publisher – Arano et al. 2023).

The experimental investigation conducted may contribute to develop simplified design methods for assessing the influence of fire exposure on the capacity of RC slabs. Furthermore, measurements of the complete load-deflection response can help to validate existing models that predict the enhancement of bending capacity due to the arch effect and its reduction after exposure to high temperatures, as well as the increased ultimate load due to the TMA. This can be useful to assess the robustness and reliability of the structural member subjected to fire exposure.

6. Blast and fire interaction tests

The combined action of fire exposure and explosion load plays an important role for the accidental load design of SFTBs. For this reason, the structural performance of RC slabs subjected to fire exposure and, subsequently, to a blast load was investigated (Colombo et al. 2021). In this study, specimens identical to those tested in static condition (RC circular slabs) were used. As for the static tests, a hydrocarbon fire curve was applied by means of a gas burner,

considering the same two fire exposure times (60 and 120 min) in addition to the unexposed reference case. The temperature distribution over cross section is like that already represented for the static tests.

Dynamic tests were then carried out in residual conditions using a shock tube device (Colombo et al. 2011) with the slab in a simply supported condition. The details of the tests set-up are represented in Figure 15. Two distinct pressure histories, referred to as LP and HP, respectively, with peak pressures of 0.35 MPa and 1.1 MPa, are depicted in Figure 16 for all the tests carried out.

It is important to note that, in the shock tube testing approach used here, the sharp increase in pressure is accompanied by a similarly rapid and significant temperature change in the air within the tube. However, during blast phenomena (such as shock wave propagation), the temperature rise occurs very quickly and lasts for a very short duration. As a result, concrete structures—due to their low thermal conductivity—are not significantly affected by these temperature variations, as they cause only negligible changes to the structural temperature profile.

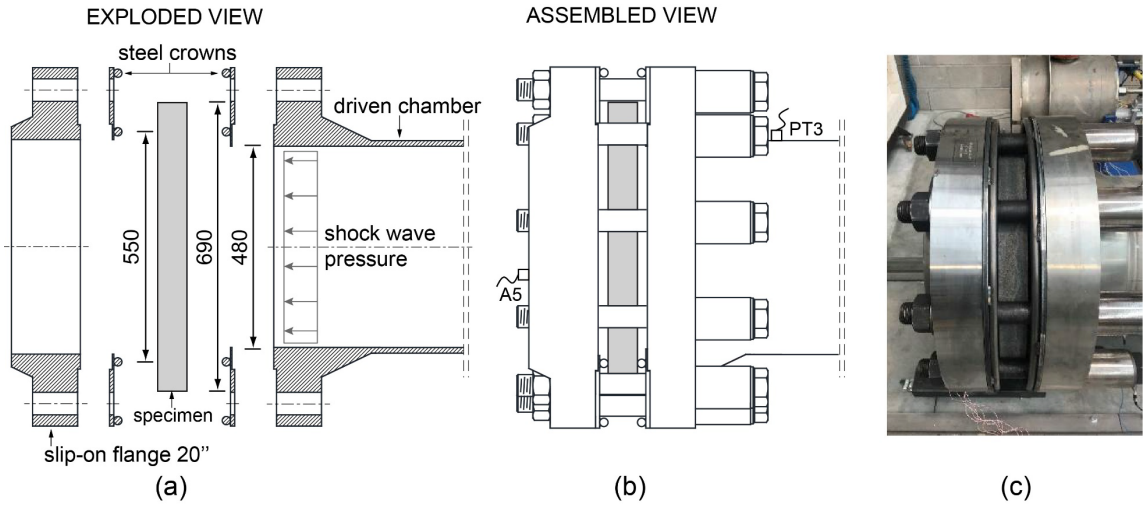

Figure 15. Details of the boundary conditions of the slab in the shock tube equipment (reprinted with the permission of the publisher – Colombo et al. 2021)

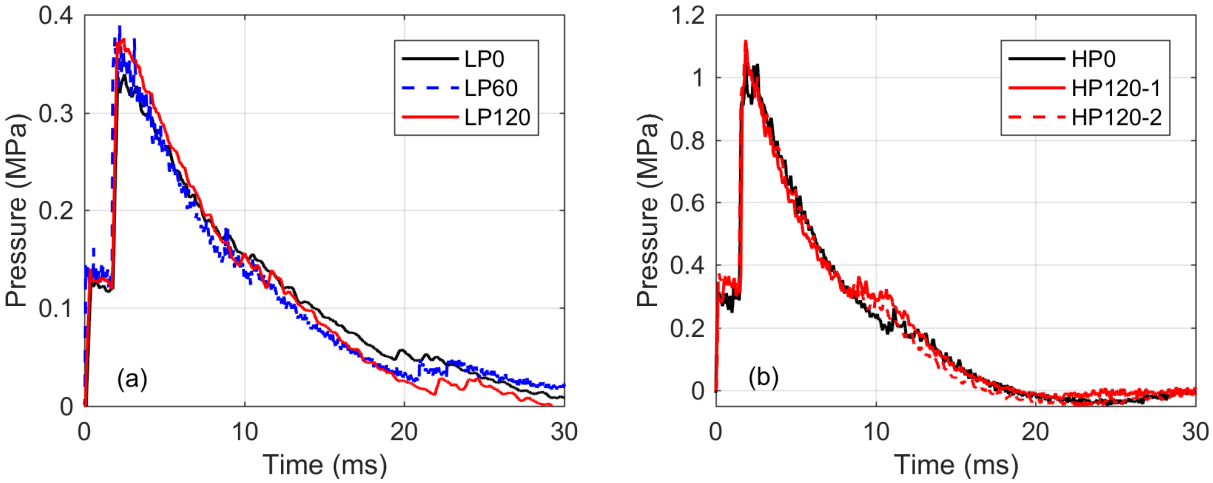

Figure 16. Pressure–time histories applied to the samples in shock tube tests (reprinted with the permission of the publisher – Colombo et al. 2021)

The specimen acceleration during the shock wave application was measured at the slab centre (A1) and at three points 120° apart, 120 mm from the centre (A2, A3, A4), as shown in Figure 17. Measurements from UPV equipment, thermocouples embedded in the specimen, and accelerometers allowed the study of high-temperature effects across the thickness and the dynamic response of the thermally damaged RC slab. Simplified numerical tools, including the Single Degree of Freedom (SDOF) model and linear elastic Finite Element (FE) analysis, were used to analyse the results.

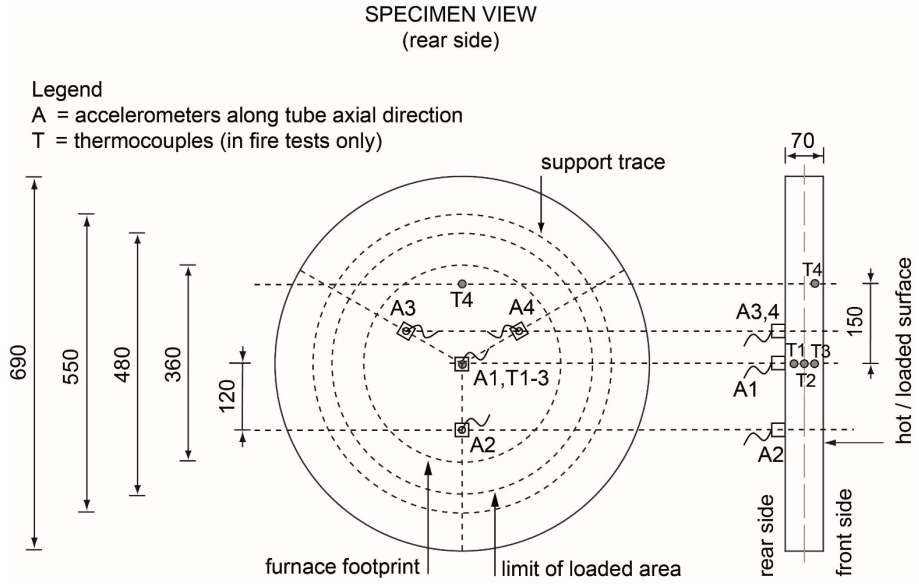

Figure 17. Sample geometry and position of accelerometers in shock tube tests (reprinted with the permission of the publisher – Colombo et al. 2021)

Results showed that thermal damage from the fire exposure causes a reduction of the overall stiffness in the RC slabs. Consequently, the main frequency of the specimen is considerably reduced, (about 50 %), thus elongating the oscillation period. Such damage in the specimen leads to a plastic state with irreversible deformations. As a result, higher energy is dissipated which leads to an increase of the damping ratio. The blast load has a relatively low effect on the main frequency of the specimen, while further increases the damping ratio. The evolution of the first natural frequency and damping with fire exposure time and blast load is shown in Figure 18. The variation in damping and natural frequency of the sample was computed through post-processing of the acceleration signal recorded from the specimens during the blast test. Specifically, the first natural frequency of the sample was derived from a Fourier transform, which provides the frequency spectrum of the response. The damping ratio was calculated by analysing the decay of the acceleration peaks during each test. More details can be found in Colombo et al. (2021). On one hand, the variation in natural frequency can be considered an indicator of the damage accumulated by the material, as it is primarily related to stiffness degradation. On the other hand, the evolution of the damping ratio is correlated with plastic strains and cracking, as suggested by Panteliou et al. (2001).

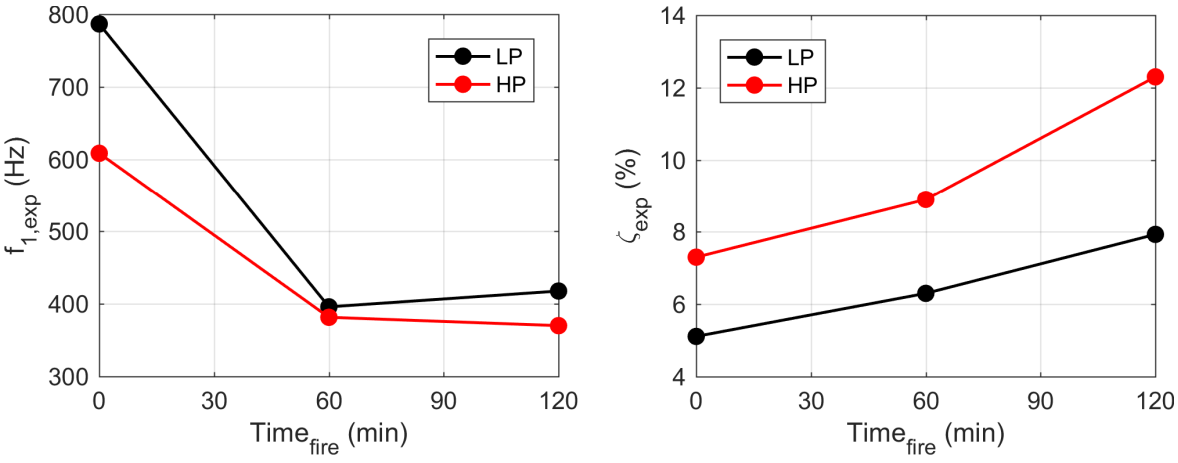

Figure 18. (a) Evolution of the first natural frequency and (b) damping of the samples when subjected to fire exposure (reprinted with the permission of the publisher – Colombo et al. 2021)

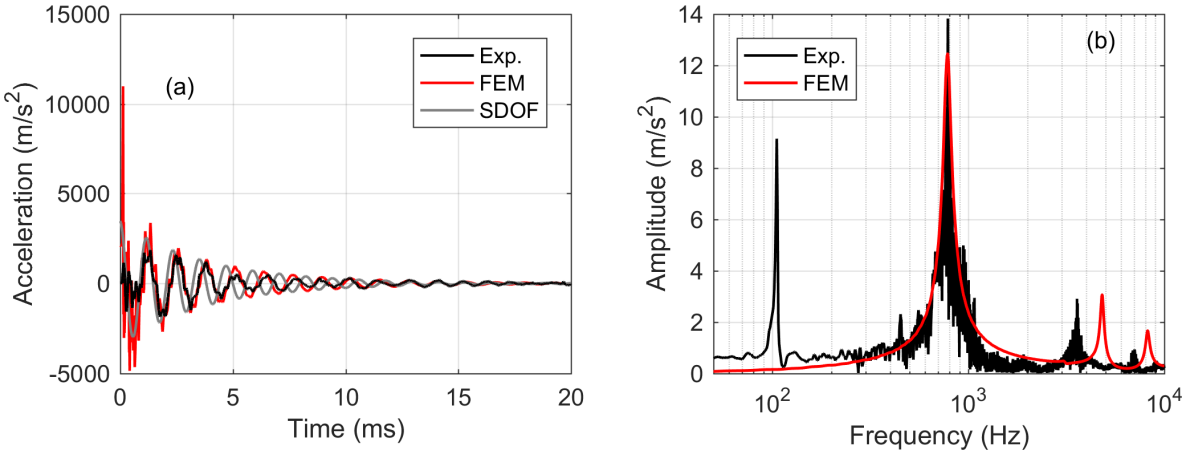

Figure 19. Acceleration response of sample LP0 – comparison between measured data and numerical approaches: (a) time history and (b) response spectrum (reprinted with the permission of the publisher – Colombo et al. 2021)

Similar measurements from three accelerometers at the same distance from the centre indicate a comparable thermal damage throughout the exposed region, despite the unevenly distributed spalling region. Results from a linear elastic FE model agree with the experimental frequency and deformation of the first mode of vibration, therefore validating the simply supported boundary conditions from the experimental test set-up (Figure 19). Moreover, similar time history acceleration values at the central point are obtained using the simplified SDOF model, although slightly overestimating the stiffness of the slab and thus showing a lower oscillation period compared to the FE model and the experimental results (Figure 19).

The FE model used here is a simple elastic model consisting of 3-node shell elements (10 mm element size; 5 integration points over the thickness), constrained by a circular bilateral support (as in the experimental setup) and subjected to a pressure history identical to that measured during the LP shock tube tests. In this model, the central point acceleration of the slab was recorded with the same sampling rate used in the experiments, and the results were used for comparison in Figure 19.

For the SDOF model, an equivalent single-degree-of-freedom system was defined, adopting an elastic deformed shape for the slab under uniform distributed load with circular

bilateral support. More details on the definition of the SDOF parameters can be found in Colombo and Martinelli (2012).

The experimental investigation presented is relevant as it contributes to the few research studies available in the literature investigating the combined effect of fire and blast on RC structures. This can provide a reliable benchmark for the development and calibration of numerical models, considering the complexity of such load scenario involving temperature and strain rate effects on the material and on the structure.

7. Conclusions

The study aimed to investigate the subsequential effect of fire exposure and blast loading on RC slabs by analysing the impact of elevated temperatures on the mechanical properties of concrete, along with carrying out static and dynamic tests on heated RC circular slabs.

The obtained constitutive behaviour of concrete material, in compression and tension, at several elevated temperatures confirm the pronounced reduction of strength and modulus of elasticity reported in the literature and in some Standards (prEN 1992-1-2, 2019; *fib* Model Code 2010, 2013), while both the strain at maximum stress and the ultimate strain increase. This result in flattened stress-strain and crack opening displacement relationships as temperature increases and indicates an overall softening of the material. The observed modification of the constitutive relationships at high temperature results in a decrease of the specific fracture energy in compression, while in an increase in uniaxial tension.

The structural mechanisms observed during the static tests of RC slabs occur also after fire exposure, although with some differences. The enhanced bending capacity attributed to the arch mechanism at small deflections is considerably affected by the fire exposure, as it is dominated by the adverse permanent damage on the compressive response of concrete. However, the strong recovery of steel after cooling leads to a similar enhanced ultimate load,

caused by the tensile membrane action (TMA), thus confirming the robustness and structural reliability of this RC slab in residual conditions. Simplified predictions using the yield-line approach, together with a good knowledge of the material at elevated temperatures, provide satisfactory results of the reduced bending capacity of the RC slab after exposure to fire.

The dynamic tests show a considerable reduction (by half) of the fundamental frequency of the RC slab after fire exposure, also resulting in an elongation of the fundamental period in the central acceleration response. This is mainly caused by the expected decrease of the stiffness at high temperatures. The softening of the material leads to a more distributed crack pattern, also enlarging the maximum amplitude of the acceleration response. Both the thermal damage and the microcracks lead to a higher dissipation of energy, (linearly) increasing the damping ratio with fire exposure. The contribution of the high-pressure of the blast load does not further significantly reduce the natural frequency of the exposed specimens. Nevertheless, the additional damage and microcracks lead to a great increase of the damping ratio. The results of SDOF and FE models agree with the experimental findings, thus proving to be useful and reliable tools to assess the dynamic response of RC slabs.

Safety considerations of concrete structures require evaluation of accidental load scenarios involving extreme load conditions. The findings of the present study are valuable to define a reliable benchmark for numerical models which, upon numerical upscaling, will be instrumental for the design of the SFTB under the exceptional case of fire exposure and blast loading.

Disclosure statement

No potential conflict of interest was reported by the authors.

References

Arano A, Colombo M, Martinelli P, Øverli JA, Hendriks MAN, Kanstad T, et al. Material

Characterization Approach for Modelling High-Strength Concrete after Cooling from Elevated Temperatures, 2021, J Mater Civ Eng n.d. https://doi.org/10.1061/(ASCE)MT.1943-5533.0003694.

Arano A., Colombo M., Martinelli P., Øverli J.A., Hendriks M.A.N., Kanstad T., di Prisco M., Failure characteristics of reinforced concrete circular slabs subsequently subjected to fire exposure and static load: An experimental study. Structural Concrete 2023; 24 (1), pp. 872 - 891

Børre S., Minoretti, A. (2014), Long Span Bridge in Norway, International Seminar on Long Span Bridge Construction, Maintenance and Disaster Resistance Techniques, Shanghai, China

Bastami M., Chaboki-Khiabani A., Baghbadrani M., Kordi M., Performance of high strength concretes at elevated temperatures, Scientia Iranica, Volume 18, Issue 5, 2011, Pages 1028-1036, ISSN 1026-3098, https://doi.org/10.1016/j.scient.2011.09.001.

Colombo M, Felicetti, R., New NDT techniques for the assessment of fire-damaged concrete structures. Fire Safety Journal, 2007, 42,6-7, https://doi.org/10.1016/j.firesaf.2006.09.002.

Colombo M, di Prisco M, Martinelli P. A New Shock Tube Facility for Tunnel Safety. Exp Mech 2011;51:1143–54. https://doi.org/10.1007/s11340-010-9430-7.

Colombo M, Martinelli P. Pressure-impulse diagrams for RC and FRC circular plates under blast loads. Eur J Environ Civ Eng 2012;16:837–62. https://doi.org/ 10.1080/19648189.2012.675149.

Colombo M, Martinelli P, Arano A, Øverli JA, Hendriks MAN, Kanstad T, et al. Experimental investigation on the structural response of RC slabs subjected to combined fire and blast. Structures 2021; 31:1017–30. https://doi.org/10.1016/j.istruc.2021.02.029.

Felicetti R, Gambarova PG, Sora MPN, Khoury GA. Mechanical behaviour of HPC and UHPC in direct tension at high temperature and after cooling. Proc. 5th Symp. Fibre-Reinforced Concr. BEFIB 2000, Lyon: 2000, p. 749–58.

Felicetti R, Gambarova PG. On the Residual Tensile Properties of High- Performance Siliceous Concrete Exposed to High Temperature. In: Pijaudier-Cabot G, Biinar Z, Gérard B, editors. Work. “Mechanics Quasi-Brittle Mater. Struct., Prague: 1999, p. 167–86.

Felicetti R, Gambarova PG. Effects of high temperature on the residual compressive strength of high-strength siliceous concretes. ACI Mater J 1998;95:395–406. https://doi.org/10.14359/382.

fib Model Code for Concrete Structures 2010. Berlin (Germany): Ernst & Sohn: 2013.

fib Bulllettin No. 96. - Guidelines for Submerged Floating Tube Bridges. Guide to good practice - 119 pages, ISBN 978-2-88394-144-1, October 2020.

Hager I, Pimienta P. Mechanical Properties of HPC at High Temperatures. Proc. Int. Work. fib Task

Group, Fire Des. Concr. Struct. What now? What next?, Milan: 2004, p. 95–100. https://doi.org/10.1007/978-94-009-1714-9_32.

ISO. (2019). ISO 15630-1:2019 Steel for the reinforcement and prestressing of concrete — Test methods. Part 1: Reinforcing bars, rods and wire. International Organization for Standardization.

Janotka I, Bágel L. Pore structures, permeabilities, and compressive strengths of concrete at temperatures up to 800°C. ACI Mater J 2002;99:196–200. https://doi.org/10.14359/11713.

Khoury GA, Algar S, Felicetti R, Gambarova PG. Mechanical behaviour of HPC and UHPC concretes at high temperatures in compression and tension. ACI Int. Conf. "State-of-the-Art High Perform. Concr., Chicago: 1999.

Kristoffersen, M.; Hauge, K.O.; Minoretti, A.; Børvik, T. Experimental and numerical studies of tubular concrete structures subjected to blast loading. Eng. Struct. 2021, 233, 111543.

Lam E.S., Fang S., Direct Tensile Behavior of Normal-Strength Concrete at Elevated Temperatures, Materials Journal, Volume 111, Issue 6, 2014, Pages 641-650, DOI: 10.14359/51686915

Minoretti A, Xiang X, Johansen IL, Eidem M. The Future of the Tunnel Crossing: The Submerged Floating Tube Bridge. Struct Eng Int 2020:1–5 https://doi.org/10.1080/10168664.2020.1775165.

Morita, T., Saito, H., Kumagai, H. (1992) Residual Mechanical Properties of High-strength Concrete Members Exposed to High Temperature. Part 1: Test on Material Properties. In Proc. Summaries of Technical Papers of Annual Meeting. Niigata, Japan: Architectural Institute of Japan.

Nakamura H, Higai T. Compressive fracture energy and fracture zone length of concrete. In: Shing PB, Tanabe T-A, editors. Model. Inelast. Behav. RC Struct. under Seism. Loads, Reston, VA: ASCE: 2001, p. 471–87.

Noumowe, A., P. Clastres, G. Debicki, and J. L. Costaz. 1996. "Transient heating effect on high strength concrete." Nucl. Eng. Des. 166 (1): 99–108. https://doi.org/10.1016/0029-5493(96)01235-6.

Panteliou SD, Chondros TG, Argyrakis VC, Dimarogonas AD. Damping factor as an indicator of crack severity. J Sound Vib 2001;241:235–45. https://doi.org/ 10.1006/jsvi.2000.3299.

Phan LT, Carino NJ. Mechanical Properties of High-Strength Concrete at Elevated Temperatures. Gaithersburg (USA): 2001.

Poon, C. S., S. Azhar, M. Anson, and Y. L. Wong. 2001. "Comparison of the strength and durability performance of normal- and high-strength pozzolanic concretes at elevated temperatures." Cem. Concr. Res. 31 (9): 1291–1300. https://doi.org/10.1016/S0008-8846(01)00580-4

prEN 1992-1-2:2019-10. Eurocode 2: Design of concrete structures – Part 1-2: General – Structural fire design. CEN/TC 250/SC 2/WG 1; 2019.

Ruan Z, Chen L, Fang Q. Numerical investigation into dynamic responses of RC columns subjected for fire and blast. J Loss Prev Process Ind 2015;34:10–21. https://doi.org/10.1016/j.jlp.2015.01.009.

Sancak E, Sari YD, Simsek O. Effects of elevated temperature on compressive strength and weight loss of the light-weight concrete with silica fume and superplasticizer. Cem Concr Compos 2008;30:715–21. https://doi.org/10.4324/9780203071236.

Zhai C, Chen L, Xiang H, Fang Q. Experimental and numerical investigation into RC beams subjected to blast after exposure to fire. Int J Impact Eng 2016;97:29–45. https://doi.org/10.1016/j.ijimpeng.2016.06.004.

Zhang Q, Wang W, Bai S, Tan Y. Response analysis of tunnel lining structure under impact and fire loading. Adv Mech Eng 2019;11:1–6. https://doi.org/10.1177/1687814019834473.